Neurobiology of Disease 124 (2019) 176–182

Contents lists available at ScienceDirect

Neurobiology of Disease

journal homepage: www.elsevier.com/locate/ynbdi

Decreased pallidal vesicular monoamine transporter type 2 availability in Parkinson's disease: The contribution of the nigropallidal pathway

Sang Soo Cho[a,b,c], Leigh Christopher[c,d], Yuko Koshimori[c,e], Crystal Li[c], Anthony E. Lang[a], Sylvain Houle[c], Antonio P. Strafella[a,b,c,*]

[a] The Edmond J. Safra Program in Parkinson's Disease & Movement Disorder Unit, Toronto Western Hospital, University Health Network, University of Toronto, Ontario, Canada
[b] Krembil Research Institute, University Health Network, University of Toronto, Ontario, Canada
[c] Research Imaging Centre, Campbell Family Mental Health Research Institute, Centre for Addiction and Mental Health, University of Toronto, Ontario, Canada
[d] Department of Neurology and Neurological Sciences, FIND Lab, Stanford University, Stanford, CA, USA
[e] Music and Health Research Collaboratory (MaRC), Faculty of Music, University of Toronto, Toronto, Ontario, Canada

ARTICLE INFO

Keywords:
Dopamine
Globus pallidus
Parkinson's disease
Positron emission tomography
Vesicular monoamine transporter type 2

ABSTRACT

To date, the contribution of the nigropallidal pathway degeneration to Parkinson's disease (PD) motor symptoms has received little attention and is generally poorly understood in spite of solid evidence that the globus pallidus (GP) receives a dense neuronal projection from the substantia nigra. To explore the dopaminergic (DA) changes of the GP in PD, we measured the availability of vesicular monoamine transporter 2 (VMAT2) using [^{11}C]DTBZ and positron emission tomography in 30 PD patients and 12 controls. PD patients were classified in two groups based on severity of disease. VMAT2 reduction was found to be significant in the external GP (GPe) regardless of the disease stage, while the internal GP (GPi) showed reduction only in more severe patients. Pallidal VMAT2 binding correlated with dopaminergic changes in the striatum, with the GPe showing a stronger association than GPi. Our findings showed DA terminals in the GPe and GPi may be differentially vulnerable in different stages of the disease, possibly playing a distinctive role in the development of motor complications with GPi DA deficiency contributing more to later-stage symptoms.

1. Introduction

Parkinson's disease (PD) is the second most common neurodegenerative disease after *Alzheimer's disease* (Alves et al., 2008). Histopathologically, PD is characterized by a severe loss of dopaminergic neurons in the substantia nigra pars compacta (SNc) (Ehringer and Hornykiewicz, 1960; Marsden, 1982) and accumulation of α-synuclein in Lewy bodies and Lewy neurites (Spillantini et al., 1997) leading to a progressive disruption in motor control with development of resting tremor, rigidity and bradykinesia.

As a pathological hallmark of PD, the nigrostriatal dopamine (DA) projections from SNc to striatum along with their axonal degeneration have been well investigated over the years (Burke and O'Malley, 2013 for review; Hornykiewicz, 1998). In contrast, much less attention has been paid to the contribution of the nigro-pallidal dopaminergic pathway, and the understanding on its role in PD is more limited. The globus pallidus (GP), as a major output structure of the basal ganglia, is critically involved in the regulation of voluntary movement. This important structure receives dense neuronal dopaminergic projections from the SNc and the ventral tegmental area (VTA) as well (Beukema et al., 2015; Cossette et al., 1999; Parent et al., 1990; Parent and Smith, 1987). In particular, dopaminergic terminals from the VTA project predominantly to ventral pallidum (Deutch et al., 1988; Klitenick et al., 1992), forming the mesopallidal dopaminergic pathway involved in motivational processing (Melendez et al., 2004); whereas dopamine innervation to the dorsal GP originates predominantly from neurons in the SNc (Hattori et al., 1975; Prensa & Parent, 2001), forming the nigropallidal dopaminergic pathway, involved in the "indirect-pathway" controlling motor inhibition (Delong et al., 1985). Pathological changes of the nigro-pallidal pathway in PD have been suggested in animal model, where lesions to the SNc caused decrease of DA in GP (Parent et al., 1990). Other studies using deterministic tractography in PD have showed changes in connectivity measures, with an increase in mean diffusivity and radial diffusivity of the nigro-pallidal pathway and a

* Corresponding author at: Toronto Western Hospital/Krembil Research Institute, CAMH-Research Imaging Centre, University of Toronto, Toronto, ON M5T 2S8, Canada.
E-mail addresses: antonio.strafella@uhn.ca, antonio.strafella@camh.ca (A.P. Strafella).

https://doi.org/10.1016/j.nbd.2018.11.022
Received 6 September 2018; Received in revised form 1 November 2018; Accepted 20 November 2018
Available online 22 November 2018

relation with disease severity scores (Tan et al., 2015).

The GP is segmented into external (GPe) and internal (GPi) parts and the functions of two substructures are distinguishable by neuronal firing patterns and rates (Delong et al., 1985; Sterio et al., 1994), distribution of DA receptor types (Camps et al., 1989; Richfield et al., 1987) and other neurotransmitters (Haber and Elde, 1981). The observed differences between GPe and GPi are consistent with different anatomical connections and functional roles of the two segments (Jaeger and Kita, 2011; Parent and Hazrati, 1995), which also suggests distinct biological changes with disease progression in PD.

Presynaptic dopaminergic integrity can be measured in several ways including the type 2 vesicular monoamine transporter (VMAT2). VMAT2 is responsible for the storage of monoamine neurotransmitters, such as dopamine (DA), into synaptic vesicles, and typically it is sensitive to changes in vesicular DA concentration (De La Fuente-Fernandez et al., 2003). The activity of this presynaptic monoaminergic binding site is proposed to be less prone to changes induced by medication or compensatory mechanisms compared to L-aromatic amino acid decarboxylase activity or dopamine transporter binding (Arena and Stoessl, 2016), and thus it is believed to be a more objective biomarker of dopaminergic terminal integrity (Frey et al., 1996).

[^{11}C]-dihydrotetrabenazine ([^{11}C]DTBZ) has been used as reliable in-vivo radioligand for imaging VMAT2 density and distribution (Chan et al., 1999; Koeppe et al., 1996). Reduced striatal DTBZ and its relationship with clinical measures has been reported in 1-methyl-4-phenyl-l,2,3,6-tetrahydropyridine (MPTP) induced Parkinsonism model of non-human primate (Blesa et al., 2010) as well as in PD patients (Bohnen et al., 2006; Frey et al., 1996). There is limited information in the literature about VMAT2 changes in the region of GP in PD patients. To fill this knowledge gap, we extended our investigation to this important region (i.e. GP). In particular, we assessed VMAT2 binding using [^{11}C]DTBZ PET to investigate functional changes in the presynaptic DA nerve terminals of the caudate, putamen and the two GP subregions in patients with PD. First, we quantified changes in the nigro-pallidal dopaminergic pathway measuring sub-regional changes of the GP and possible relation with disease severity. Second, we intended to confirm previous observation of nigrostriatal dopaminergic degeneration in PD and its association with disease severity related changes. Finally, we investigated the relationship between VMAT2 bindings in each region of interest and clinical measure of disease severity.

2. Methods

2.1. Patients

Thirty PD patients (12 females; age 69.7 ± 6.3, range 56–80 yrs) meeting UK Brain Bank criteria for the diagnosis of idiopathic PD patients and 12 age- and education-matched healthy controls (HC, 10 females; age 65.7 ± 4.1, range 58–79 yrs) were identified for this study. Participants underwent clinical assessment, [^{11}C]DTBZ positron emission tomography (PET) and structural MRI scan on separate days to avoid excessive fatigue after providing written informed consent (Christopher et al., 2015; Christopher et al., 2014).

PD patients were divided into two groups based on severity of disease, assessed while on medication ("ON" state) with their usual anti-parkinsonian drugs; i.e. PD1, patients with H & Y stage 1.5–2 and PD2, patients, with H & Y stage 2.5–3. All anti-parkinsonian medications were stable for at least one month prior to study enrolment. At the time of study entry, 28 PD patients were receiving levodopa (Levodopa/Carbidopa n = 27; Levodopa/Benserazide, n = 1), 2 patients were on non-levodopa medication. Medical assessments were conducted in the morning time, and patients were asked to take their dose of dopaminergic medication at least 1 h before their appointment. Parkinsonian disability was assessed using the modified Hoehn and Yahr (H & Y) Rating Scale (Goetz et al., 2004) and the Unified Parkinson Disease Rating Scale motor score (UPDRS III) during the on-medication state. Levodopa equivalent daily dose (LEDD) for each patient was calculated based on Tomlinson et al. (2010). Montreal Cognitive Assessment (MoCA) and Beck depression inventory (BDI) were obtained in all participants to measure general cognitive capabilities and depression levels, respectively.

Patients with a history of other neurological diseases, psychiatric illness, or any medical condition that precluded them from PET imaging were excluded from the study. None of the normal subjects had a history of neurological, psychiatric, or major medical diseases. For the healthy controls, MoCA and BDI score were included as inclusion/exclusion criteria, any participant who had < 26 in MoCA and > 14 in BDI were excluded. The study protocol was approved by the Research Ethics Committees, at the Centre for Addiction and Mental Health and the University Health Network of the University of Toronto.

2.2. [^{11}C]DTBZ PET image

[^{11}C]DTBZ was prepared as described previously (Jewett et al., 1997). Radiochemical purities were > 98%. The PET scans were obtained using a 3D high-resolution research tomograph (HRRT) brain scanner (CS/Siemens, Knoxville, TN, USA), which measures radioactivity in 207 slices with an interslice distance of 1.22 mm. The detectors of the HRRT are a LSO/LYSO phoswich detector, with each crystal element measuring 2 × 2 × 10 mm^3. Patients were imaged after overnight withdrawal (12h) of their antiparkinsonian medications, to ensure to standardize effect of medication while patients are still functional (Defer et al., 1999). To minimize subject's head movements in the PET scanner, we used a custom-made thermoplastic facemask together with a head-fixation system (Tru-Scan Imaging, Annapolis). A 10-min transmission scan, measured using a single photon point source, 137Cs ($t_{1/2}$ = 30.2 years, Eγ = 662 keV) was acquired immediately before the acquisition of the emission scan for attenuation correction. After the transmission scan, the [^{11}C]DTBZ was injected as a bolus into an intravenous line placed in an antecubital vein. Emission data were acquired in list mode for 60 min while subjects were at rest.

The emission list mode data were rebinned into a series of 3D sinograms. The 3D sinograms were gap-filled, scatter corrected and Fourier rebinned into 2D sinograms. The images were reconstructed from the 2D sinograms using a 2D filtered-back projection algorithm, the reconstructed image has 256 × 256 × 207 cubic voxels measuring 1.22 × 1.22 × 1.22 mm^3. The dynamic images were reconstructed into 17 frames: The first frame was of variable length being dependent on the time between the start of acquisition and the arrival of [^{11}C]DTBZ in the tomograph FOV. The subsequent frames were defined as 1 × ≥22 s, 4 × 60 s, 3 × 120 s, 8 × 300 s, 1 × 600 s.

Whole-brain T1-weighted and diffusion-weighted images were acquired using a 3.0 T GE Signa HD × MRI system (General Electric, Milwaukee, WI) equipped with an eight-channel phased array head coil. A high-resolution three-dimensional (3D) anatomical scan was acquired with a T1-weighted 3D IR-FSPGR sequence (TR/TE/TI, 7.8/min full/450 ms; matrix, 256 × 256; voxel size, 1 × 1 × 1 mm; field of view, 256 × 256 mm; flip angle, 15°; 180 axial slices), used for anatomical references for PET analysis.

2.3. Voxel-based parametric PET image analysis

After the pre-registration procedure, parametric [^{11}C]DTBZ PET binding potential (BP) map was calculated in the native PET space with simplified reference tissue method (Lammertsma and Hume, 1996) using the occipital cortex time activity curve value as reference. For voxel-based statistical analysis, parametric BP images were transformed into standardized stereotaxic space using individual MRI. Finally, normalized images were smoothed with a Gaussian function at 8 mm full width half-maximum. The image preprocessing for the statistical analysis was carried out with SPM 12 (Wellcome Department of Imaging

Neuroscience, London). Based on a priori hypothesis, the voxel-wise analysis was restricted over a brain volume corresponding to the basal ganglia. A height threshold of false discovery rate (FDR) corrected $P < .05$ and an extent threshold of 20 voxels was used for generating the initial t-map to determine the predicted peaks and visualization. Percent (%) changes of each significant brain regions were extracted within the significant cluster using anatomical ROIs. The local maxima of each cluster were expressed in the Montreal Neurological Institute (MNI) coordinates.

2.4. ROI-based parametric PET image analysis

The brain regions corresponding to the bilateral putamen, caudate, external globus pallidus (GPe) and internal globus pallidus (GPi) were included for the region-of-interest (ROI). Values for each ROIs were taken from the individual BP map and used for all statistical analysis. ROIs were obtained from WFU-PickAtlas toolbox (http://www.fmri.wfubmc.edu/cms/software) and transformed into a parametric [^{11}C]DTBZ BP map, and the [^{11}C]DTBZ BP was extracted using Matlab based REX toolbox (http://web.mit.edu/swg/software.htm) (Supplementary Fig. S1). The location of GPi and GPe in each PET image was confirmed by PET co-registered and segmented T1 and T2-weighted MRI using overlay function in Mango (http://rii.uthscsa.edu/mango/).

2.5. Statistical analysis

For the demographic comparisons among three groups, we used one-way analysis of variance (ANOVA) and for comparisons of clinical measures between the two PD groups, Student's *t*-test was applied. Gender distribution in three groups was tested by chi-square test.

For the ROI analysis, VMAT2 availability was compared with 2-way mixed ANOVA and MoCA score included as covariate. If a significant main effect/interaction was found, pair-wise comparison of post hoc tests (FDR correction for multiple comparison) was applied to test for group differences. We also conducted a correlation analysis to test relationship between clinical measures associated with PD severity (i.e. disease duration, H & Y scale and UPDRS) and % decreases of regional [^{11}C]DTBZ BP in PD. For this, percentage differences from the mean [^{11}C]DTBZ BP of HCs were calculated for each PD patient in each ROIs. Pearson's partial correlation analysis (two-tailed) was used for this analysis with MoCA score as covariate. All the statistical analyses were performed in SPSS v16.0 for Windows (IBM Corp., Somers, NY, USA) with significance level at $P < .05$. All data were expressed as mean ± standard deviation (s.d.) in the tables.

3. Results

The demographic and clinical features of each group are summarized in Table 1. As expected, there was a significant difference in term of disease severity between the two groups of patients [H&Y stage score ($t = 9.02$, $P < .001$), UPDRS III ($t = 2.81$, $P < .01$), disease duration ($t = 2.23$, $P < .05$)] with the most severe PD group receiving higher levodopa equivalent daily dose [LEDD ($t = 2.29$, $P < .05$)]. There were no differences among groups in age ($F_{2,42} = 1.53$, $P = .23$), years of education ($F_{2,43} = 2.12$, $P = .09$) and BDI ($F_{2,43} = 0.34$, $P = .72$). However, there were differences in the MoCA ($F_{2,43} = 8.79$, $P < .001$) with both PD groups showing lowered level of general cognitive function compared with healthy controls (Christopher et al., 2015; Christopher et al., 2014).

Fig. 1 shows the group mean of [^{11}C]DTBZ binding in HC and two PD groups in standard stereotactic space. The group of patients with less severe disease (i.e. PD1) showed decreased [^{11}C]DTBZ binding in the bilateral GPe compared with HC [48.7% (± 24.6)], but no significant differences were noted at the level of the GPi (Table 2, Fig. 2). In contrast, the more severe group of patients (i.e. PD2) showed a more diffuse decrease in [^{11}C]DTBZ binding not only in the GPe [65.5% (± 13.4)] but also in the GPi [44.3% (± 27.3)] compared with HC (Table 2, Fig. 2). These binding reductions paralleled the well expected changes in [^{11}C]DTBZ binding in the bilateral striatum which was significantly reduced compared with HCs (Table 2), i.e. the less severe group (i.e. PD1) decreased by 38.7% (S.D = ± 25.1) in the caudate and 58.3% (± 22.9) in the putamen; the more severe group (i.e. PD2) decreased by 57.6% (± 16.9) in the caudate and 76.6% (± 9.6) in the putamen.

Table 1
Demographics and clinical characteristics of Parkinson's disease (PD) patients and healthy control (HC) participants.

	HC	PD 1	PD 2
Age (yr)	65.7 (4.1)	68.3 (7.0)	71.0 (5.2)
Gender (female/male)	10FM/2M	10FM/8M	2FM/10M[§]
Education (yr)	17.7 (2.6)	16.7 (2.2)	15.3 (1.7)
MoCA	28.3 (1.3)	25.1 (3.0) [+]	23.1 (3.1)[++]
BDI	3 (1.8)	4.1 (3.1)	3.8 (3.5)
Hoehn and Yahr stage	–	1.9 (0.2)	2.6 (0.1)[**]
UPDRS III	–	21.7 (11.6)	35.4 (15.1)[**]
Disease Duration (yr)	–	4.5 (3.1)	8.5 (4.1)[*]
LEDD (mg/day)	–	454.5 (268.6)	742.7 (427.0)[*]
Levodopa[§]	–	n = 16	n = 12
Total daily levodopa dose	–	382.8 (235.4)	666.7 (389.4)[*]
Injected mass (μg)	1.4 (0.6)	1.5 (1.2)	1.5 (0.7)
Specific activity (mCi/μmol)	2762.7 (1231.6)	2601.6 (982.4)	2301.9 (800.9)

All data are expressed as mean (s.d.); PD1 vs PD2: [*]P < .05, [**]P < .001, HC vs PD1 or PD2: [+]P < .05, [++]P < .001; Fisher's Exact Chi-Square Test, HC vs PD3 [§]P < .01; BDI: Beck depression Inventory; MoCA: Montreal Cognitive Assessment; UPDRS: unified Parkinson's disease rating scale; LEDD: levodopa equivalent daily dose; §: number of patients who is taking levodopa. N.A.: not available. Values in bracket indicate standard deviation.

The ROI-based analysis was consistent with observations from voxel-based analysis (Fig. 3). Striatal sub-areas and GP sub-structures were tested separately, results from striatum are used only for display purpose. For the ROI analysis, we found significant interaction between group and sub-structure of GP ($F(2, 38) = 18.6$, $P < .001$) and significant main effect of group ($F(2, 38) = 20.9$, $P < .001$) with both PD groups showing lowered [^{11}C]DTBZ BP compared with HC. Subsequent pairwise comparisons confirmed significant decline of GP, specifically, lowered GPi BPs were found only in the more advanced group ($P = 0.03$ for left GPi; $P = .02$ for right GPi). As expected, there was a significant correlation in the severity of denervation between striatum and GP. In particular, the reduction in [^{11}C]DTBZ binding in the putamen correlated with the changes both in the GPe ($r = 0.89$, $P < .001$) and GPi ($r = 0.61$, $P < .01$), with the GPe showing a steeper correlation than GPi (Fig. 4), implying larger BP changes in the GPe than those in the GPi.

In PD patients, we found few significant correlations between [^{11}C]DTBZ changes and some clinical measures (Table 3). Higher percentage reduction in [^{11}C]DTBZ bindings was associated with longer disease duration mainly in the GPe ($P < .05$) and in striatal regions (caudate: $P < .05$; putamen: $P < .01$). The putamen showed as well a correlation between H & Y stage and % decrease in [^{11}C]DTBZ bindings.

4. Discussion

The aim of the present study was to investigate the dopaminergic changes associated with the loss of nerve terminals in the GP, and their potential contribution to disease severity in PD patients. Our findings showed a significant bilateral degeneration in the nigro-pallidal dopaminergic pathway which paralleled to certain extent the presynaptic loss in the nigro-striatal dopaminergic pathway. In particular, the loss of DA nerve terminals (i.e. reduction in VMAT2 binding) in the pallidal subregions (i.e GPe and GPi) showed some interesting differences, with the GPi affected mainly in the most severe group of patients (i.e. PD2),

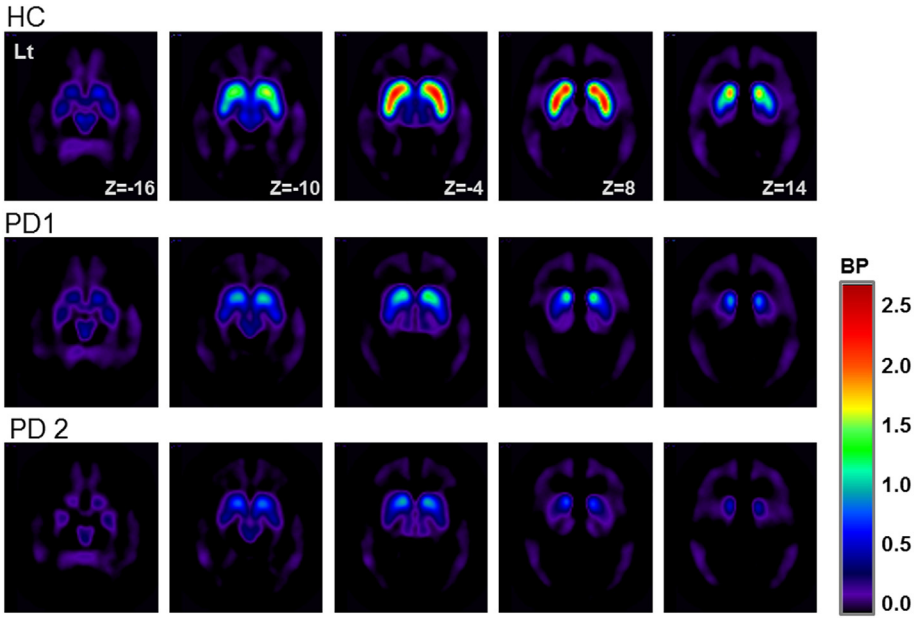

Fig. 1. Distribution of the VMAT2 in basal ganglia. Color bar indicate BPs of [^{11}C]DTBZ. The mean parametric [^{11}C]DTBZ BP maps of each groups are in MNI space (axial view). Lt: left, BP: binding potential.

Table 2
Coordinates and statistical values in the basal-ganglia structures with decreased [^{11}C]DTBZ BP in PD groups compared with HCs.

Region	MNI Coordinates (mm)			T-score	Cluster size (Voxels)
	X	Y	Z		
HC > PD1					
Lt Putamen	−30	−6	2	10.16	818
Lt Caudate	−16	16	4	5.47	
Rt Putamen	30	−4	4	9.45	612
Rt Caudate	18	18	8	5.20	
Lt GPe	−26	−12	2	6.61	170
Rt GPe	26	−10	−4	5.28	21
HC > PD2					
Lt Putamen	−26	−2	6	11.3	875
Lt Caudate	−16	16	4	7.1	
Rt Putamen	30	−8	4	10.4	647
Rt Caudate	18	18	8	5.76	
Lt GPe	−26	−12	2	7.15	235
Lt GPi	−12	0	−4	2.59	
Rt GPe	26	−10	−4	6.67	98
Rt GPi	16	−2	−4	2.70	

Lt: left, Rt: right, GPe: external globus pallidus, GPi: internal globus pallidus.

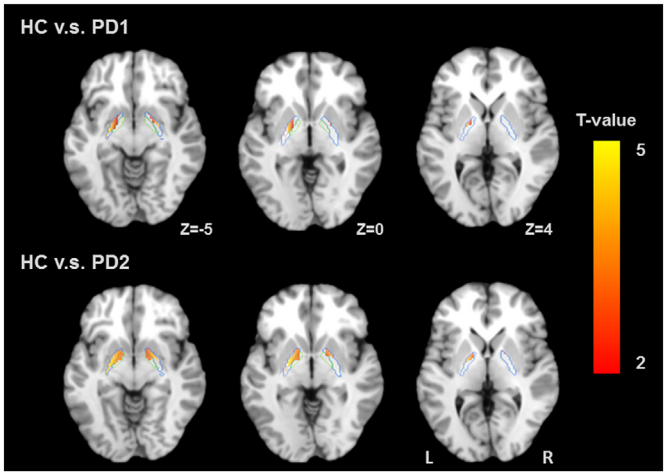

Fig. 2. Result of voxel-based parametric analysis of [^{11}C]DTBZ BP. GP substructures showing a significant decrease of [^{11}C]DTBZ BP in group PD1 (H & Y: 1.5–2) (upper row) and Group PD2 (H & Y: 2.5–3) (lower row) compared with age matched healthy controls, controlled for MoCA (FDR corrected $P < .05$, $k = 20$). Striatum was masked for display purpose. Anatomic boundaries of the GPe are marked in blue and GPi marked in green color. Lt: left, Rt: right. (For interpretation of the references to color in this figure legend, the reader is referred to the web version of this article.)

whereas dopaminergic changes in the GPe were observed as well in the group of patients with milder disease severity (i.e PD1). This pallidal DA degeneration correlated with dopaminergic changes in the striatum, with the GPe showing a stronger association than GPi. Moreover, the percentage reduction in [^{11}C]DTBZ bindings (in the GPe and striatum) was associated with longer disease duration and one measure of disease severity (i.e. H&Y stage).

There are few studies investigating dopaminergic function in GP using other dopaminergic radioligands. For example, a significantly decreased of D2/3 receptor of GP post-synaptic binding in drug-naı̈ve PD has been reported using [^{11}C]-(+)-PHNO (Boileau et al., 2009). More recently, another study showed in the GP a reduced D2/3 post-synaptic binding with [^{18}F]fallypride in patient with PD, and their motor severity was positively correlated with D2/3 receptor density in the GP(Stark et al., 2018). Only one study tested the nigropallidal pre-synaptic pathway in PD using ^{18}F-DOPA and showed disease progression related uptake changes in GP substructure. Other studies, focusing mainly on the nigrostriatal pathway, have previously shown the decrease of striatal VMAT2 availability with the progression of clinical severity in PD (Bohnen et al., 2006; Hsiao et al., 2014). Our new observations indicate that pallidal VMAT2 binding is a sensitive tool for detecting DA degeneration in the nigropallidal pathway, although VMAT2 levels are normally significantly lower than in putamen and caudate nucleus. The innervation of the pallidal region from midbrain dopaminergic neurons appears rather complicated. In non-human primate studies, dopaminergic innervation in pallidal segments was observed after injection of biotinylated dextran amine in the dopaminergic area of the midbrain (Jan et al., 2000). The injections of the retrograde fluorescent tracer fast blue in the striatum and nuclear yellow in the GPi in the squirrel monkey revealed a nigropallidal projection whose cellular origin was largely distinct from that of the

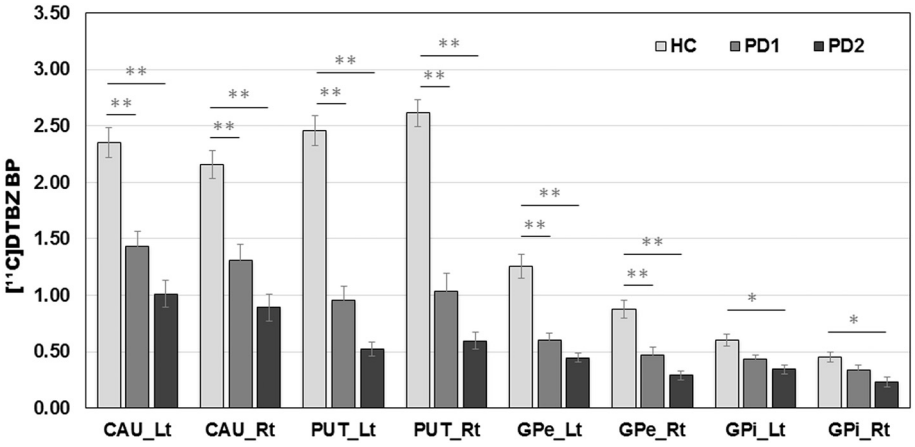

Fig. 3. The mean BP in the bilateral GPe, GPi and striatum (caudate and putamen) for HCs, PD1 and PD2. There was significant main effect of group ($F_{(2, 38)} = 20.9$, $P < .001$) with both PD groups showing lower [^{11}C]DTBZ BP compared with HCs. Lt: left, Rt: right, CAU: caudate, PUT: putamen, GPe: external globus pallidus, and GPi: internal globus pallidus. Error bars represent the standard errors of the mean. *P < .05, **P < .01 (FDR corrected for multiple comparison).

nigrostriatal pathway (Smith et al., 1989). However, other anatomical studies have also reported evidence of nigrostriatal axons providing collaterals that arborize in the pallidum (Cossette et al., 1999).

A very interesting contribution to this argument came from a postmortem study in PD brain (Rajput et al., 2008), where the authors interpreted the findings of more significant loss of DA in GPe (compared to GPi) as a result of the severe loss of pallidal collaterals from the degenerating nigrostriatal DA fibers. DA fibers innervating the GPi were suggested to be separate from both the nigrostriatal fibers and those innervating the GPe, and degenerating independently, thus supporting the more moderate DA loss in GPi. These observations are quite consistent with our results which provide additional evidence for differences in the relationship of DA terminal loss and disease severity between the two pallidal segments (GPe and GPi); VMAT2 reduction was significant in the GPe regardless of disease stage, while the GPi showed significant reduction only in more severe stages. Involvement of the nigro-GPi pathway may contribute more to later-stage motor dysfunction and possibly to the development of motor complications seen in more advanced PD. Compensatory function of DA projection to the GPi was suggested as well by Whone et al. (2003). Their findings showed that increased GPi ^{18}F-Dopa uptake in early PD and loss of activity later in the disease. They interpreted this result as a mechanism for maintaining a normal pattern of pallidal output to thalamus and proposed that reduction of the nigro-GPi dopaminergic innervation could correlate with the development of motor complications such as wearing off. The observations from Whone and colleague are however, different

Table 3
Correlation results between clinical measures and % changes of [^{11}C]DTBZ binding in PD.

	Disease duration		H&Y stage		UPDRS III	
	r	p-value	r	p-value	r	p-value
Caudate	**−0.45***	**0.01**	−0.31	0.10	−0.26	0.17
Putamen	**−0.56***	**0.002**	**−0.47***	**0.01**	−0.20	0.30
GPe	**−0.43***	**0.02**	−0.32	0.09	−0.19	0.33
GPi	−0.31	0.10	−0.17	0.40	−0.18	0.35

Bold indicates Pearson correlation, *P < .05 (two-tailed), FDR corrected.

from our results, since there was no increase of GPi VAMT2 in mild PD group. This discrepancy may be explained by the clinical stage of the patients. The early PD in previous study had much shorter disease duration (1.8 yr) than our mild PD group (4.5 yr).

Overall the literature, and our study as well, seem to suggest that DA terminals in the GPe and GPi may be differently vulnerable in PD. The reason for this intriguing observation is obviously not clear, however, neuroanatomical and neurophysiological studies may provide some insights. We know from previous reports that in addition to the traditional direct and indirect striatal pathways (Kravitz et al., 2010), several cortical areas including primary motor cortex, the supplementary motor area, the premotor, the anterior cingulate and the dorsolateral prefrontal cortex send excitatory projections to GPi via the STN, through the well-known hyperdirect pathway (Kitai and Deniau, 1981;

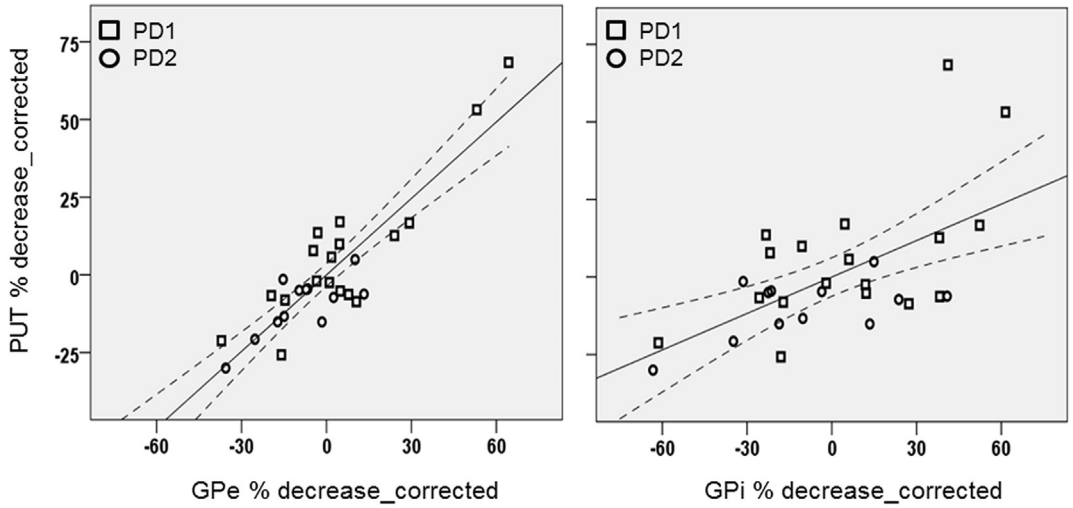

Fig. 4. Relationship between putaminal % change and pallidal % changes of [^{11}C]DTBZ BP in PD. PUT: putamen, GPe: external globus pallidus, and GPi: internal globus pallidus.

Nambu et al., 2002). The influence of this fast and very effective pathway from various cortical brain regions to GPi supports its primary role in motor control as the main output structure of the basal ganglia (Gillies et al., 2017; Herrojo Ruiz et al., 2014), where on-line top-down monitoring and adjusting of ongoing voluntary movement can be an important compensatory mechanism for maintaining more normal motor control in the early stages of PD, failing in later stages when DA terminals in the GPi start also to degenerate.

This study has certainly some limitations to consider. First, we failed to match gender in each group, the ratio of gender was significantly different. There is an argument about gender differences of dopaminergic function in PD. One study reported higher caudate nucleus dopamine transporter binding in woman compared with men (Kaasinen et al., 2015), and another other study showed that women with PD had 87% higher F-dopa uptake in the right dorsolateral prefrontal cortex compared to men with PD (Kaasinen et al., 2001). Those findings are not confirmed with larger patient cohort and gender specific variance of dopaminergic function in GP have not been reported so far. When we tested gender as a confound factor, the main effect of group ($P < .001$) and interaction ($P < .001$) were still significant, pairwise comparison between HC and PD1 was lowered to trend level only in the right GPi ($P = .075$). Although our main result was still maintained after controlling for gender in the additional analysis, further studies are needed to test also gender specific effect on disease progress and its relationship of dopaminergic function in GP and its substructure using larger sample. Another limitation factor to consider is that clinical measures in our PD patients were obtained while on-medication; thus, the relationship between severity of motor symptoms and DA degeneration in the GP sub-region is not properly represented. Although we showed a relationship between dopaminergic function in GP and disease duration, investigating the relationship between motor features (tested "on" as well as "off" state) and changes of VMAT 2 with disease progression could provide more supportive evidence on the contribution of GP in development of PD motor symptoms.

We tested the VMAT 2 level in the substructure of GP which is a small structure. Traditionally, PET imaging has always suffered of lower spatial resolution compared to other imaging modality such as MRI, in particular when it comes to spill- over effect in small structure (Harri et al., 2007). Using HRRT scanner with small detector size enhanced sensitivity, reduced partial-volume effect (PVE) (van Velden et al., 2009), however there are still an argument related with balancing noise and signal level. Noise level usually can be controlled by adapting spatial filtering during and after image reconstruction, however use of filtering cost of lower spatial resolution(Sakaguchi et al., 2008). In this study, the ROI location was confirmed with PET image co-registered MRI, the smoothing kernel that we used for Gaussian filtering (8 mm full width half-maximum) was much smaller than our ROI size, and our ROI results conducted using nonsmoothed BP map well matched with results from voxel-based analysis. Combining this with the benefit of using a HRRT scanner, we think the effect of PVE is quite small in current results if any.

In conclusion, our finding of decreased VMAT2 availability in pallidal nuclei suggests an important role of the nigropallidal pathway in the contribution of motor symptoms in PD. Both imaging and anatomical studies seem to suggest that there are differences in the DA terminal loss between the two pallidal segments (GPe and GPi) related to disease severity with dopaminergic degeneration found to be present in the GPe regardless of the disease stage, while that in the GPi appears only in more severe stages; thus, possibly contributing to the development of motor problems seen in more advanced PD.

Supplementary data to this article can be found online at https://doi.org/10.1016/j.nbd.2018.11.022.

Author contributions

A.P·S. and S.S.C. conceived and designed the study. S.S.C., L.C., Y.K., C.L., and A.P.S contributed to data collection and analysis of imaging data. S.S.C., A.E.L., S.H., and A.P.S. contributed to writing and drafting the manuscript.

Competing interests

The authors declare that they have no competing interests.

Acknowledgement

This work was supported by Canadian Institutes of Health Research (MOP-136778) to Dr. Antonio Strafella. Dr. A Strafella is supported by Canada Research Chair Program.

References

Alves, G., et al., 2008. Epidemiology of Parkinson's disease. J. Neurol. 255 (Suppl. 5), 18–32.
Arena, J.E., Stoessl, A.J., 2016. Optimizing diagnosis in Parkinson's disease: Radionuclide imaging. Parkinsonism Relat. Disord. 22, S47–S51.
Beukema, P., et al., 2015. In vivo characterization of the connectivity and subcomponents of the human globus pallidus. NeuroImage 120, 382–393.
Blesa, J., et al., 2010. Progression of dopaminergic depletion in a model of MPTP-induced Parkinsonism in non-human primates. An (18)F-DOPA and (11)C-DTBZ PET study. Neurobiol. Dis. 38, 456–463.
Bohnen, N.I., et al., 2006. Positron emission tomography of monoaminergic vesicular binding in aging and Parkinson disease. J. Cereb. Blood Flow Metab. 26, 1198–1212.
Boileau, I., et al., 2009. Decreased binding of the D3 dopamine receptor-preferring ligand [11C]-(+)-PHNO in drug-naive Parkinson's disease. Brain 132, 1366–1375.
Burke, R.E., O'Malley, K., 2013. Axon degeneration in Parkinson's disease. Exp. Neurol. 246, 72–83.
Camps, M., et al., 1989. Dopamine receptors in human brain: autoradiographic distribution of D2 sites. Neuroscience 28, 275–290.
Chan, G.L., et al., 1999. Reproducibility studies with 11C-DTBZ, a monoamine vesicular transporter inhibitor in healthy human subjects. J. Nucl. Med. 40, 283–289.
Christopher, L., et al., 2014. Combined insular and striatal dopamine dysfunction are associated with executive deficits in Parkinson's disease with mild cognitive impairment. Brain 137, 565–575.
Christopher, L., et al., 2015. Salience network and parahippocampal dopamine dysfunction in memory-impaired Parkinson disease. Ann. Neurol. 77, 269–280.
Cossette, M., et al., 1999. Extrastriatal dopaminergic innervation of human basal ganglia. Neurosci. Res. 34, 51–54.
De La Fuente-Fernandez, R., et al., 2003. VMAT2 binding is elevated in dopa-responsive dystonia: visualizing empty vesicles by PET. Synapse 49, 20–28.
Defer, G.L., et al., 1999. Core assessment program for surgical interventional therapies in Parkinson's disease (CAPSIT-PD). Mov. Disord. 14, 572–584.
Delong, M.R., et al., 1985. Primate globus pallidus and subthalamic nucleus: functional organization. J. Neurophysiol. 53, 530–543.
Deutch, A.Y., et al., 1988. Telencephalic projections of the A8 dopamine cell group. Ann. N. Y. Acad. Sci. 537, 27–50.
Ehringer, H., Hornykiewicz, O., 1960. Distribution of noradrenaline and dopamine (3-hydroxytyramine) in the human brain and their behavior in diseases of the extrapyramidal system. Klin. Wochenschr. 38, 1236–1239.
Frey, K.A., et al., 1996. Presynaptic monoaminergic vesicles in Parkinson's disease and normal aging. Ann. Neurol. 40, 873–884.
Gillies, M.J., et al., 2017. The cognitive role of the globus pallidus interna; insights from disease states. Exp. Brain Res. 235, 1455–1465.
Goetz, C.G., et al., 2004. Movement Disorder Society Task Force report on the Hoehn and Yahr staging scale: status and recommendations. Mov. Disord. 19, 1020–1028.
Haber, S., Elde, R., 1981. Correlation between Met-enkephalin and substance P immunoreactivity in the primate globus pallidus. Neuroscience 6, 1291–1297.
Harri, M., et al., 2007. Evaluation of partial volume effect correction methods for brain positron emission tomography: Quantification and reproducibility. J. Med. Phys. 32, 108–117.
Hattori, T., et al., 1975. Demonstration of a pallido-nigral projection innervating dopaminergic neurons. J. Comp. Neurol. 162, 487–504.
Herrojo Ruiz, M., et al., 2014. Involvement of human internal globus pallidus in the early modulation of cortical error-related activity. Cereb. Cortex 24, 1502–1517.
Hornykiewicz, O., 1998. Biochemical aspects of Parkinson's disease. Neurology 51, S2–S9.
Hsiao, I.T., et al., 2014. Correlation of Parkinson disease severity and 18F-DTBZ positron emission tomography. JAMA Neurol. 71, 758–766.
Jaeger, D., Kita, H., 2011. Functional connectivity and integrative properties of globus pallidus neurons. Neuroscience 198, 44–53.
Jan, C., et al., 2000. Dopaminergic innervation of the pallidum in the normal state, in MPTP-treated monkeys and in parkinsonian patients. Eur. J. Neurosci. 12, 4525–4535.
Jewett, D.M., et al., 1997. A simple synthesis of [11C]dihydrotetrabenazine (DTBZ). Nucl. Med. Biol. 24, 197–199.
Kaasinen, V., et al., 2001. Increased frontal [(18)F]fluorodopa uptake in early Parkinson's disease: sex differences in the prefrontal cortex. Brain 124, 1125–1130.
Kaasinen, V., et al., 2015. Effects of aging and gender on striatal and extrastriatal [123I]

FP-CIT binding in Parkinson's disease. Neurobiol. Aging 36, 1757–1763.
Kitai, S.T., Deniau, J.M., 1981. Cortical inputs to the subthalamus: intracellular analysis. Brain Res. 214, 411–415.
Klitenick, M.A., et al., 1992. Topography and functional role of dopaminergic projections from the ventral mesencephalic tegmentum to the ventral pallidum. Neuroscience 50, 371–386.
Koeppe, R.A., et al., 1996. Kinetic evaluation of [11C]dihydrotetrabenazine by dynamic PET: measurement of vesicular monoamine transporter. J. Cereb. Blood Flow Metab. 16, 1288–1299.
Kravitz, A.V., et al., 2010. Regulation of parkinsonian motor behaviours by optogenetic control of basal ganglia circuitry. Nature 466, 622–626.
Lammertsma, A.A., Hume, S.P., 1996. Simplified reference tissue model for PET receptor studies. NeuroImage 4, 153–158.
Marsden, C.D., 1982. Basal ganglia disease. Lancet 2, 1141–1147.
Melendez, R.I., et al., 2004. Involvement of the mesopallidal dopamine system in ethanol reinforcement. Alcohol 32, 137–144.
Nambu, A., et al., 2002. Functional significance of the cortico-subthalamo-pallidal 'hyperdirect' pathway. Neurosci. Res. 43, 111–117.
Parent, A., Hazrati, L.N., 1995. Functional anatomy of the basal ganglia. II. The place of subthalamic nucleus and external pallidum in basal ganglia circuitry. Brain Res. Brain Res. Rev. 20, 128–154.
Parent, A., Smith, Y., 1987. Differential dopaminergic innervation of the two pallidal segments in the squirrel monkey (Saimiri sciureus). Brain Res. 426, 397–400.
Parent, A., et al., 1990. The dopaminergic nigropallidal projection in primates: distinct cellular origin and relative sparing in MPTP-treated monkeys. Adv. Neurol. 53, 111–116.
Prensa, L., Parent, A., 2001. The nigrostriatal pathway in the rat: A single-axon study of the relationship between dorsal and ventral tier nigral neurons and the striosome/matrix striatal compartments. J. Neurosci. 21, 7247–7260.
Rajput, A.H., et al., 2008. Globus pallidus dopamine and Parkinson motor subtypes: clinical and brain biochemical correlation. Neurology 70, 1403–1410.
Richfield, E.K., et al., 1987. Comparative distribution of dopamine D-1 and D-2 receptors in the basal ganglia of turtles, pigeons, rats, cats, and monkeys. J. Comp. Neurol. 262, 446–463.
Sakaguchi, K., et al., 2008. An iterative reconstruction using median root prior and anatomical prior from the segmented mu-map for count-limited transmission data in PET imaging. Ann. Nucl. Med. 22, 269–279.
Smith, Y., et al., 1989. Evidence for a distinct nigropallidal dopaminergic projection in the squirrel monkey. Brain Res. 482, 381–386.
Spillantini, M.G., et al., 1997. [alpha]-Synuclein in Lewy bodies. Nature 388, 839–840.
Stark, A.J., et al., 2018. [(18)F]fallypride characterization of striatal and extrastriatal D2/3 receptors in Parkinson's disease. Neuroimage Clin. 18, 433–442.
Sterio, D., et al., 1994. Neurophysiological properties of pallidal neurons in Parkinson's disease. Ann. Neurol. 35, 586–591.
Tan, W.Q., et al., 2015. Deterministic tractography of the nigrostriatal-nigropallidal pathway in Parkinson's disease. Sci. Rep. 5, 17283.
Tomlinson, C.L., et al., 2010. Systematic review of levodopa dose equivalency reporting in Parkinson's disease. Mov. Disord. 25, 2649–2653.
van Velden, F.H., et al., 2009. HRRT versus HR+ human brain PET studies: an inter-scanner test-retest study. J. Nucl. Med. 50, 693–702.
Whone, A.L., et al., 2003. Plasticity of the nigropallidal pathway in Parkinson's disease. Ann. Neurol. 53, 206–213.